Electronic Supplementary Material (ESI) for Physical Chemistry Chemical Physics.

Supplementary Information for:

Prediction of Capture and Utilization of Atmospheric Toxic Gases by Azo-based Square Pillared Fluorinated MOF

D.Muthukumar [a], Athulya S. Palakkal [b] and Renjith S. Pillai*[c]

[a]*Department of Chemistry, CHRIST (Deemed to be University), Bengaluru-560029, Karnataka, India*

[b]*Department of Chemistry, Faculty of Engineering and Technology, SRM Institute of Science and Technology, Kattankulathur-603 203, Chennai, India*

[c]*Analytical and Spectroscopy Division, Vikram Sarabhai Space Center, Indian Space Research Organisation, Thiruvananthapuram – 695022, Kerala, India*

Email: renjithspillai@gmail.com/ renjith_sp@vssc.gov.in

1.Crystalline Structures of FE/ALFFIVE with 4,4'-azopyridine organic linker

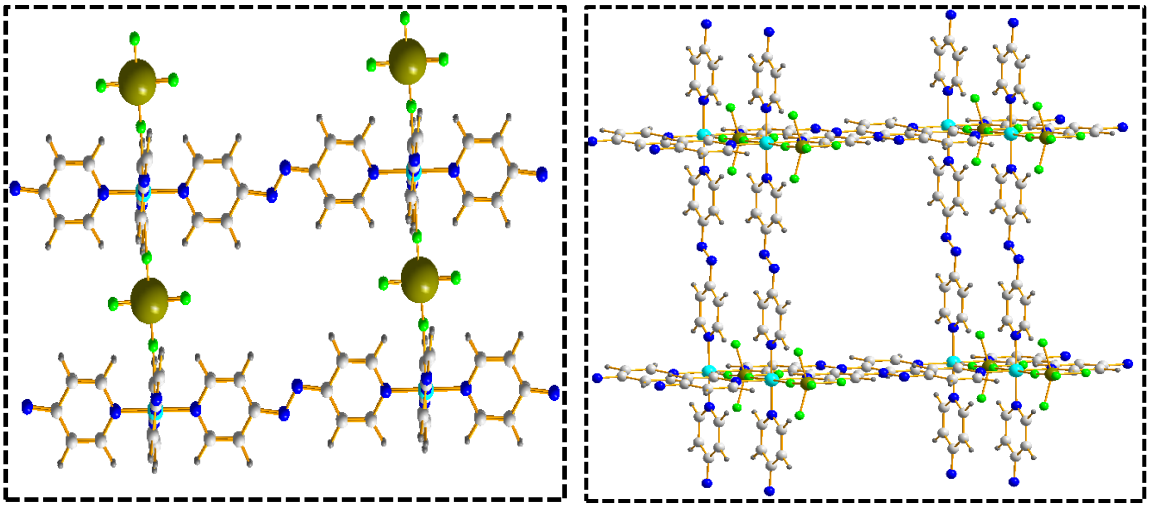

Figure S1: Unit crystal structure of MFFIVE-Ni-Apy, M=Fe/Al obtained through optimization via DFT method viewed along *a* (left) and *b* (right) vector direction.(Colour code: C; black, H; grey, N; blue, F; green, Fe/Al; olive)

2. Density Functional Theory (DFT) Calculations

The given MFFIVE-Ni-Apy where optimized with the help of PBE[1] functional in CP2K[2] package. The FEFFIVE-Ni-Apy and ALFFIVE-Ni-Apy with H_2O molecule loaded were optimized initially with Unrestricted Kohn-sham (UKS)[3] including spin multiplicity and further analyzed the optimized structure and details are given below (Table S1). A triple zeta (TZVP-MOLOPT)[4] is used for the element such as carbon, nitrogen, oxygen and fluorine, whereas nickel and Iron/Aluminium followed by a double zeta (DZVP-MOLOPT)[4] basis set, additionally includes Vander Waals corrections in DFT-D3 method[5].

Table S1: Cell parameters of H_2O-loaded Crystalline Structures of MFFIVE-Ni-Apy

MOF	Lattice Size(Å)			Angle(^{0})			Cell volume(Å^3)	Energy (eV)
	a	b	c	α	β	γ		
FEFFIVE-Ni-Apy	12.8466	12.8466	8.7620	90	90	90	1445.903	-616.459
ALFFIVE-Ni-Apy	12.8480	12.8480	8.8550	90	90	90	1461.705	-1049.795

3.Pore size distribution and specific surface area calculations

The pore size distribution of FEFFIVE-Ni-Apy and ALFFIVE-Ni-Apy were calculated by Gelb and Gubbins methodology[6], as shown in Figure S2.Additionally calculated the surface area (Figure S3) of optimized structures with the help of Gelb and Gubbins methodology[6].

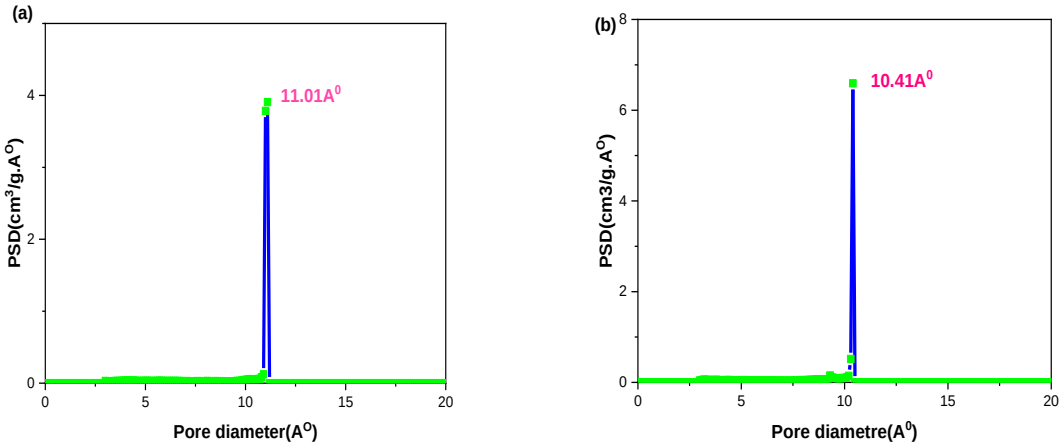

Figure S2: Pore size distribution of DFT-optimised (a) FEFFIVE-Ni-Apy and (b) ALFFIVE-Ni-Apy.

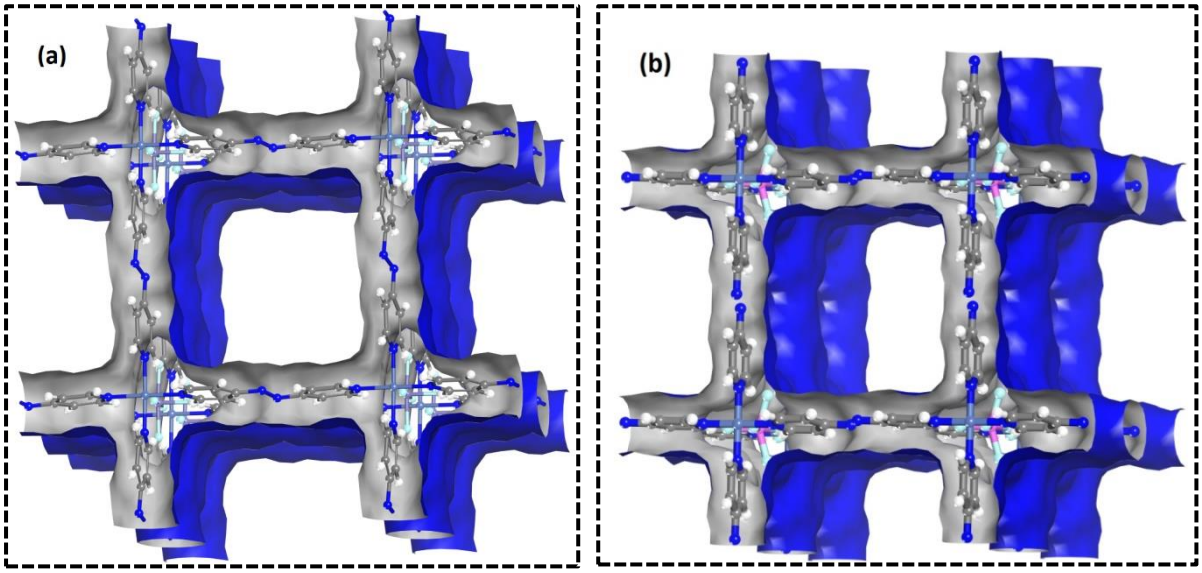

Figure S3: Surface area for optimized structures of (a) FEFFIVE-Ni-Apy and (b) ALFFIVE-Ni-Apy.

4. Interatomic Potentials (Combination of Generic Force Field and Derived Force Field)

The Guest-Host interactions are explained through the combination of Generic force field as well as the derived force field from Buckingham analytic function. Initially, the LJ parameters (Table S2) of inorganic terms were explained with the help of UFF[7] and organic part by DREIDING[8] potentials. Herein the Guest to Metal (Fe/Al) interactions is explained with the aid of specially defined derived force field (Table S3). In this work CO_2 were modelled by EPM2[9], NO_2 from the work of Bourasseau *et al*[10] model and SO_2 from used model of Potoff *et al*[11].

Table S2: LJ potential parameters for the atoms of the MFFIVE-Ni-Azpy series.

Atomic type	LJ	
	σ (A^O)	**Ɛ/K_B (K)**
C	3.473	47.857
H	2.846	7.649
N	3.662	34.724
F	3.093	38.975
Ni	2.834	7.5483
Fe	2.912	6.5419
Al	1.447	108.998

5. GCMC Simulations- Using DFT-Derived FF.

The Grand Canonical Monte Carlo simulations were performed to carry out the single component adsorption isotherm of acidic gases such as CO_2, NO_2 and SO_2 at 298K by using RASPA code[12]. The model corresponds to adsorbate and the dispersion forces in short ranges explained with the help of Lennard–Jones potential parameters and Ewald method[13] was applied for coulombic interaction with in the cut-off of 12 Å. The fugacity of species was calculated via Peng-Robinson equation of states[14]. The adsorption enthalpy (ΔH) calculated based on the NVT ensemble by using revised Wisdom's test particle insertion method[15]. Initially, MFFIVE-Ni-Apy were analysed the H_2O adsorption capacity in dry condition and further saturated with the water and this structure were optimized and performed all the adsorption processes (Loaded structure or relaxed structure). Additionally the stability of MFFIVE –Ni-Apy was performed in various percentage of humidity level at 298K and plotted the selectivity of SO_2/CO_2, NO_2/CO_2 and SO_2/NO_2 in various humidity rates.

5.1 Force field parameterization for MFFIVE-Ni-Apy (M=Fe/Al) frame work *vs* guest interaction profile.

The interatomic potential for describing Guest-Host interactions in presence of humidity is derived by quantum mechanically, whereas the initial step of calculating binding energy of framework with adsorbate via equation 1,

$$E_{B.E} = E_{MOF+Guest} - E_{MOF} - E_{Guest} \qquad (1)$$

Where E $_{(MOF+Guest)}$ corresponds to the energy of optimized metal organic framework with loaded guest molecule and E $_{MOF}$ and E $_{Guest}$ indicates the energy of MOF and guest molecule individually. The interatomic distance between Fe/Al to framework varies with a distance of 0.1 to 5A^0 and results the potential energy curve. The potential energy curve further evaluates for the derivation of new force field parameters to represent guest-host interaction. Grand canonical Monte Carlo (GCMC) was performed to determine the single component adsorption and adsorption enthalpy of guest molecule such as CO_2, NO_2 and SO_2 at 298K. Additionally binary adsorption, adsorption in presence of water was performed.

While derive force field by using Buckingham analytical function,

$$U_{ij} = \underbrace{\sum_{\substack{i,j \\ i<j}} \frac{1}{4\pi\varepsilon_0} \frac{q_i q_j}{r_{ij}}}_{\text{Electrostatic term}} + \underbrace{4\varepsilon_{ij}\left[\left(\frac{\sigma_{ij}}{r_{ij}}\right)^{12} - \left(\frac{\sigma_{ij}}{r_{ij}}\right)^{6}\right]}_{\text{Lennard-Jones term}} + \underbrace{\left[A_{ij}e^{-B_{ij}r_{ij}} - S_g\frac{C_{ij}}{r_{ij}^6}\right]}_{\text{Buckingham term}}$$

A, B and C are the conventional Buckingham parameters for repulsive and attractive contribution respectively and Sg indicates the global scaling factor for the dispersion energies. The DFT derived energy profile represented in FigureS4 and Table S3.

(a) CO_2

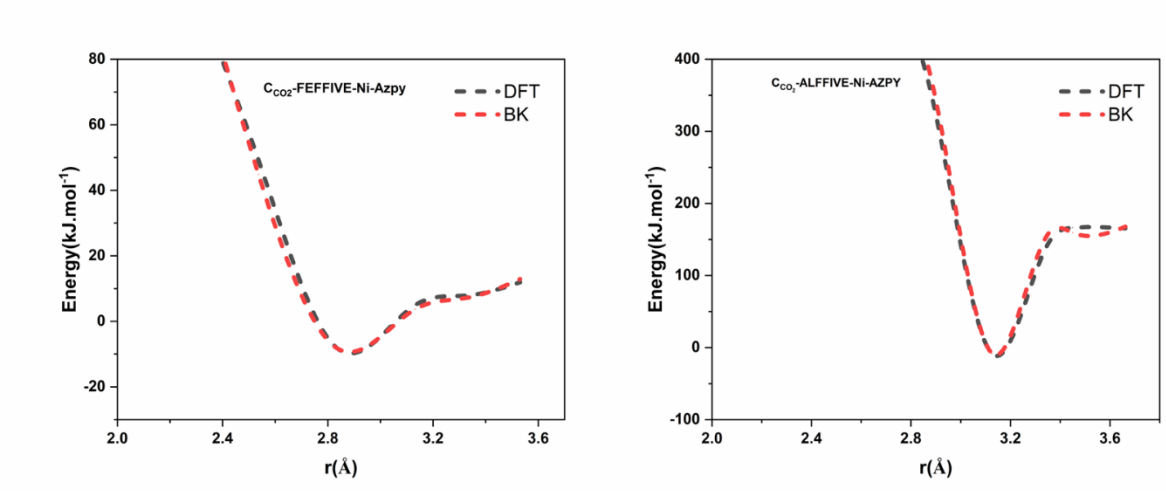

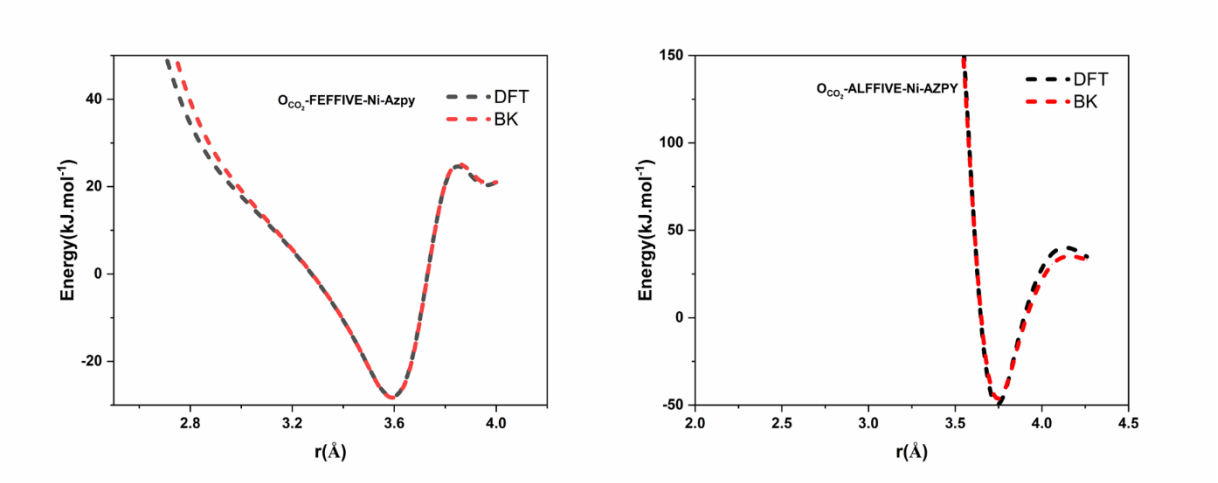
O_{CO_2}-FEFFIVE-Ni-Azpy
DFT
BK
Energy(kJ.mol^{-1})
r(Å)
O_{CO_2}-ALFFIVE-Ni-AZPY
DFT
BK
Energy(kJ.mol^{-1})
r(Å)

(b) NO_2

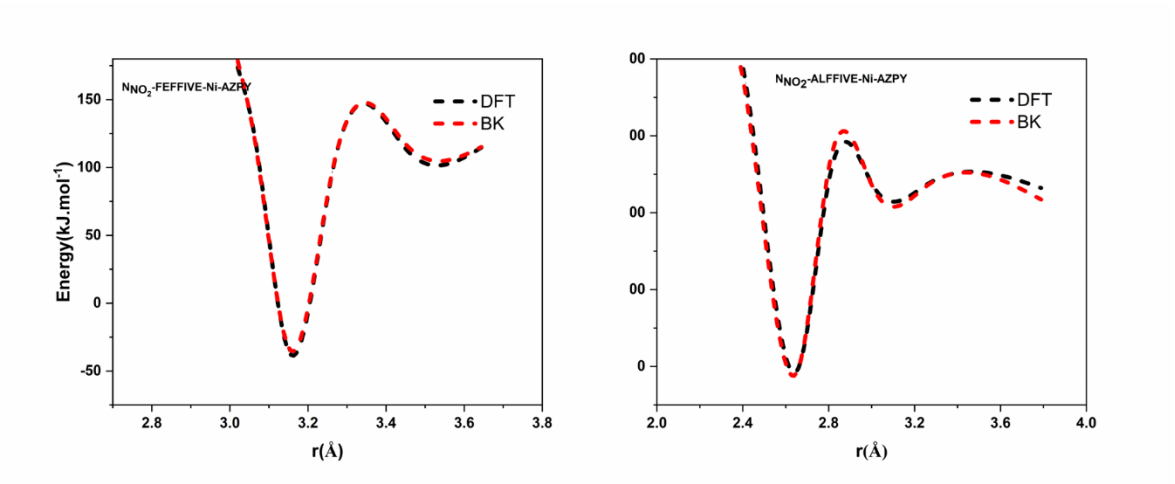
N_{NO_2}-FEFFIVE-Ni-AZPY
DFT
BK
Energy(kJ.mol^{-1})
r(Å)
N_{NO_2}-ALFFIVE-Ni-AZPY
DFT
BK
r(Å)

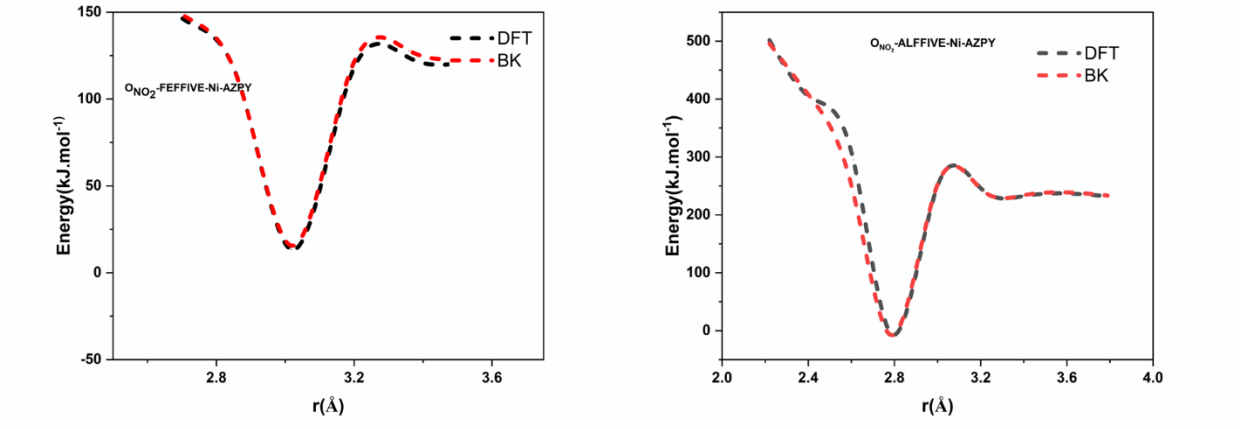
O_{NO_2}-FEFFIVE-Ni-AZPY
DFT
BK
Energy(kJ.mol^{-1})
r(Å)
O_{NO_2}-ALFFIVE-Ni-AZPY
DFT
BK
Energy(kJ.mol^{-1})
r(Å)

(c) SO_2

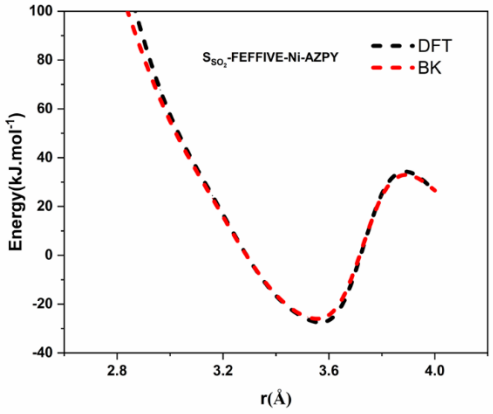
S_{SO_2}-FEFFIVE-Ni-AZPY
DFT
BK
Energy(kJ.mol^{-1})
r(Å)

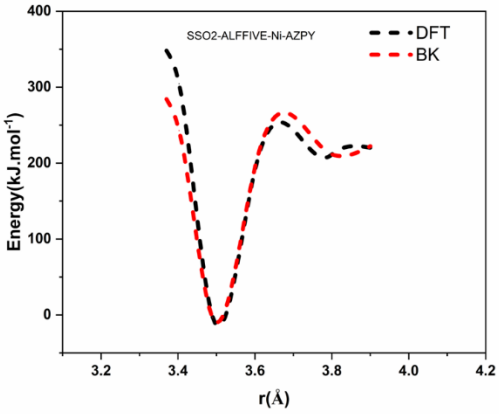
SSO2-ALFFIVE-Ni-AZPY
DFT
BK
Energy(kJ.mol^{-1})
r(Å)

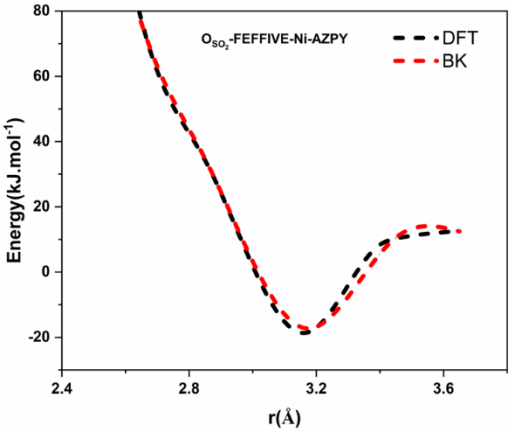
O_{SO_2}-FEFFIVE-Ni-AZPY
DFT
BK
Energy(kJ.mol^{-1})
r(Å)

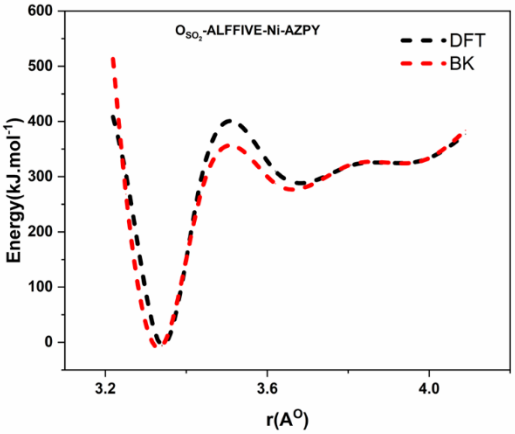
O_{SO_2}-ALFFIVE-Ni-AZPY
DFT
BK
Energy(kJ.mol^{-1})
r(A^O)

(d) H_2O

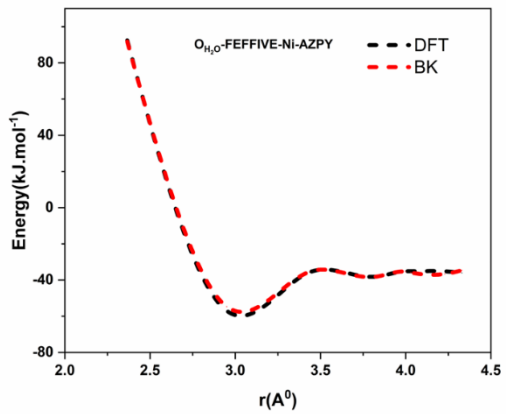
O_{H_2O}-FEFFIVE-Ni-AZPY
DFT
BK
Energy(kJ.mol^{-1})
r(A^0)

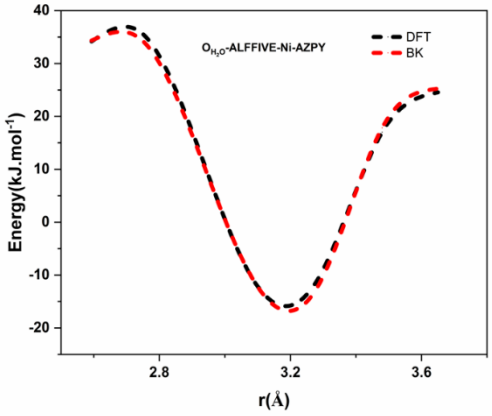
O_{H_2O}-ALFFIVE-Ni-AZPY
DFT
BK
Energy(kJ.mol^{-1})
r(Å)

Figure S4: Comparison of DFT-Derived FF fitted curve (red circles) on the DFT interaction energy profile (black squares) for FEFFIVE-Ni-Apy (left) and ALFFIVE-Ni-Apy (right) towards the CO_2 (a), NO_2 (b), SO_2 (c) and H_2O (d) guest molecule.

Table S3: Buckingham parameters associated with the MFFIVE-Ni-Apy with Adsorbates.

MFFIVE-Ni-Apy	A (kJ/mol)	B $(A^0)^{-1}$	C kJ mol^{-1} $A^{0\,6}$)
C_CO_2 –Fe	1.02e6	2.91	9.27e4
O_CO_2 -Fe	6.18e4	2.41	1e3
N_NO_2 –Fe	5.77e5	2.31	9.88e2
O_NO_2 –Fe	4.56e5	2.58	9.90e2
S_SO_2 –Fe	4.69e6	3.23	1e3
O_SO_2 –Fe	6.63e5	2.99	1e3
O_H_2O -Fe	6.51e7	4.41	1e3
C_CO_2 –Al	5.88e7	2.13	2.67e7
O_CO_2 –Al	1.12e5	2.57	1e3
N_NO_2 –Al	1.28e6	1.98	1.20e6
O_NO_2 –Al	8.37e5	2.31	1e3
S_SO_2 –Al	2.04e6	2.35	1e3
O_SO_2 –Al	8.96e5	2.1	1e3
O_H_2O -Al	9.25e5	2.06	8.33e5

6. Comparison of the Enthalpy of adsorption

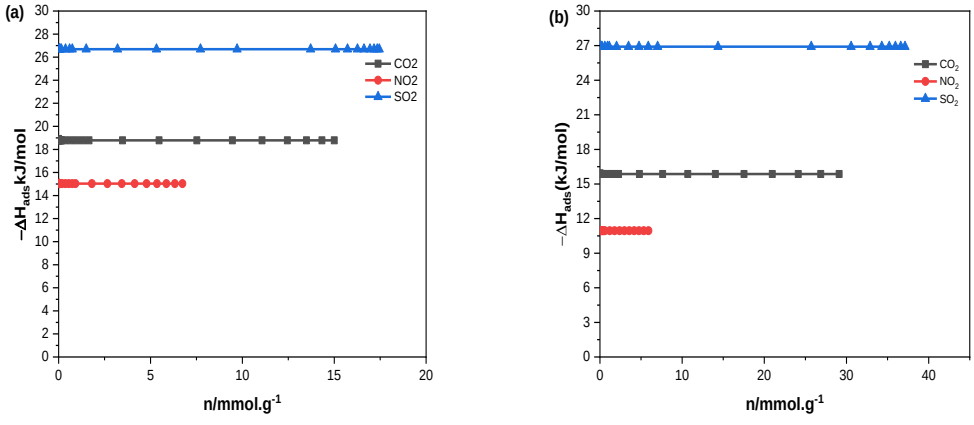

Figure S5: Enthalpy of adsorption for CO_2 (black), NO_2 (red) and SO_2 (blue) of FEFFIVE-Ni-Apy (a) and ALFFIVE-Ni-Apy (b) at 298K.

6.1 Comparison of Enthalpy of Adsorption and Binding energy

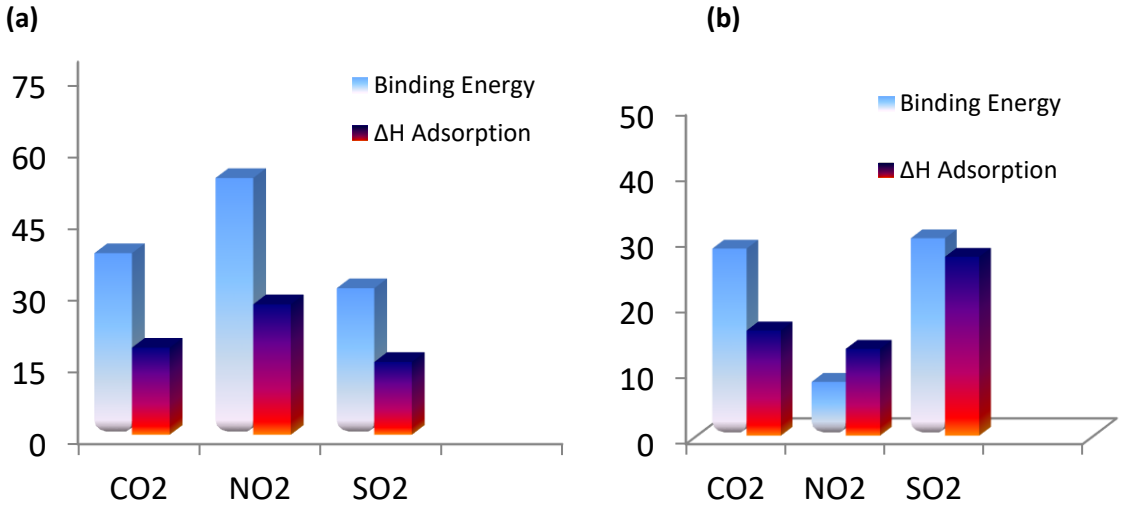

Figure S6: Comparison between DFT binding energy calculated with PBE functional (BE) and GCMC enthalpy of adsorption at 298K (ΔH) for CO_2, NO_2 and SO_2 for FEFFIVE-Ni-Apy (a) and ALFFIVE-Ni-Apy (b).

6.2 Adsorption Isotherm of H_2O

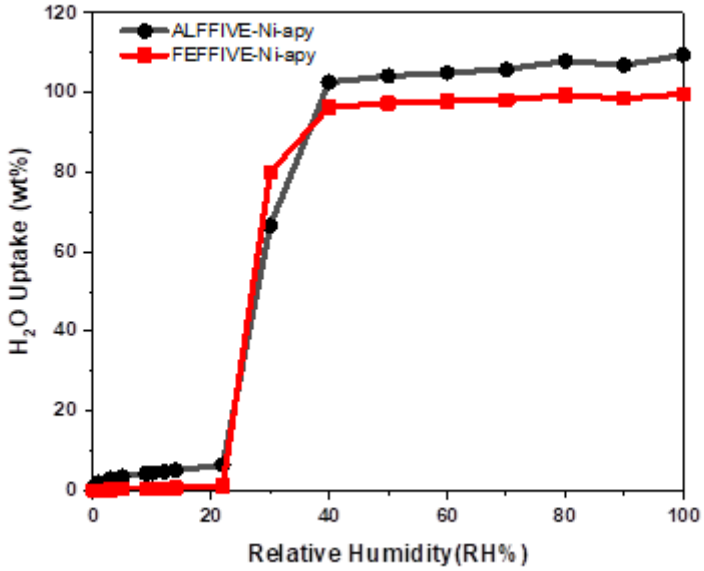

Figure S7: Single component adsorption isotherm of MFFIVE-Ni-Apy with H_2O at 298K.

7. Simulated adsorption isotherm for MFFIVE-Ni-apy at higher temperatures

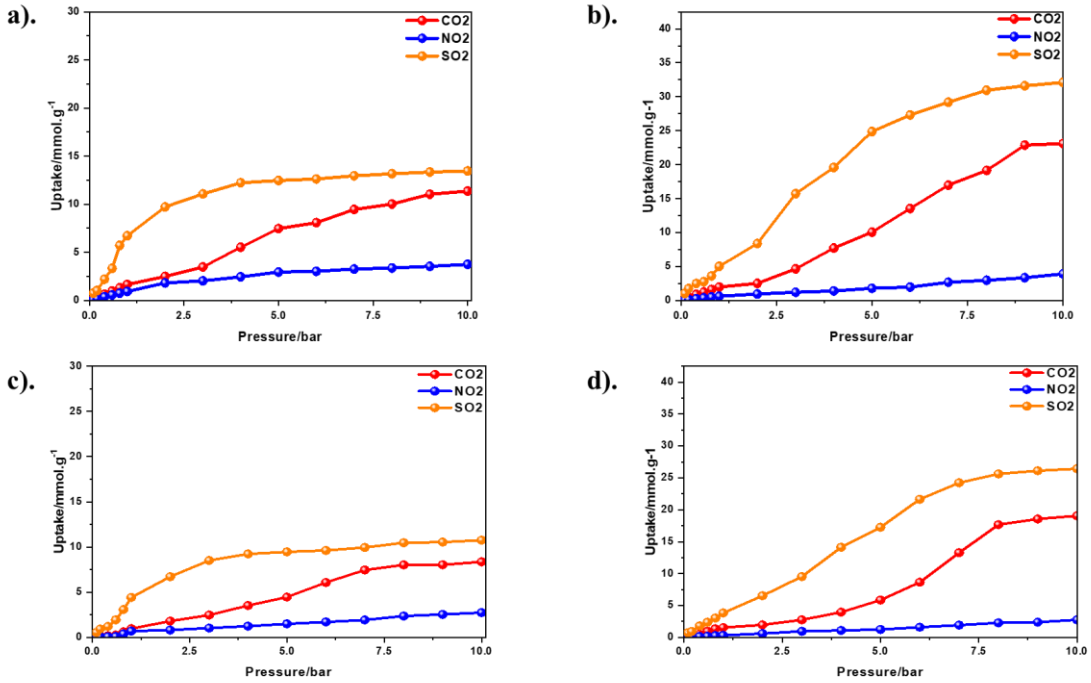

Figure S8: Single component adsorption isotherm of FEFFIVE-Ni-apy (a), (c) and ALFFIVE-Ni-apy (b), (d) at 350 K temperature and 400 K respectively.

8. Radial Distribution Functions calculated for single component adsorption

(a) CO_2

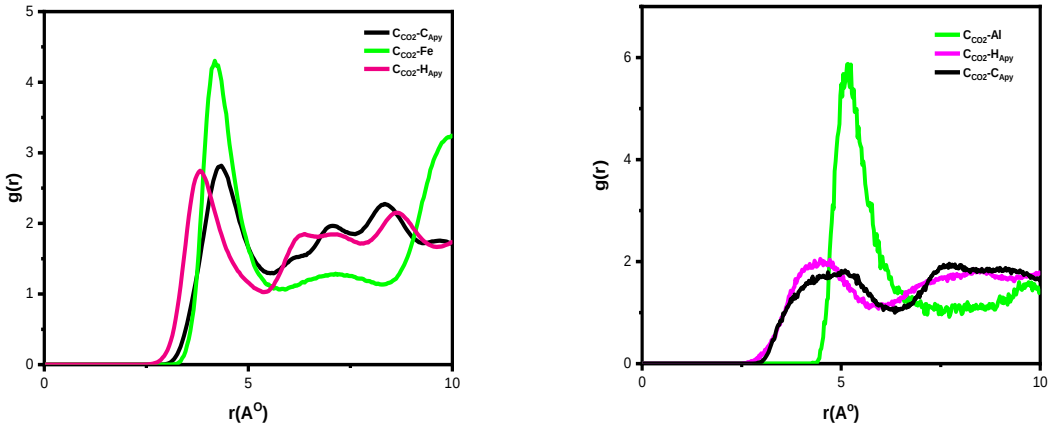

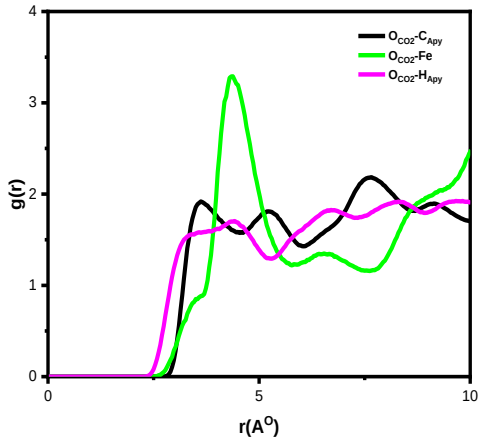
O_{CO2}-C_{Apy}
O_{CO2}-Fe
O_{CO2}-H_{Apy}
g(r)
r(A^O)

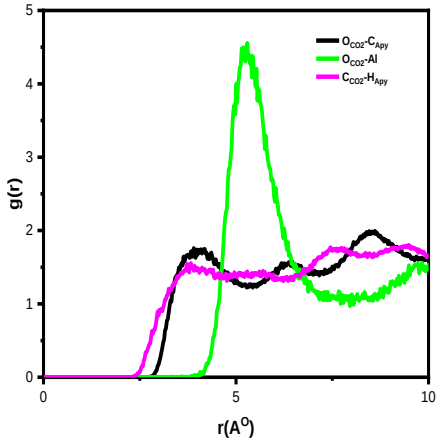
O_{CO2}-C_{Apy}
O_{CO2}-Al
C_{CO2}-H_{Apy}
g(r)
r(A^O)

(b). NO_2

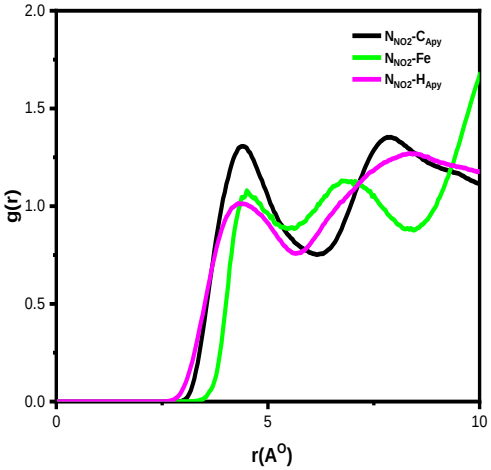
N_{NO2}-C_{Apy}
N_{NO2}-Fe
N_{NO2}-H_{Apy}
g(r)
r(A^O)

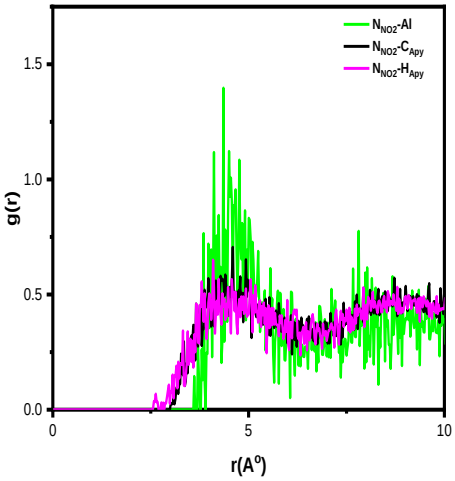
N_{NO2}-Al
N_{NO2}-C_{Apy}
N_{NO2}-H_{Apy}
g(r)
r(A^O)

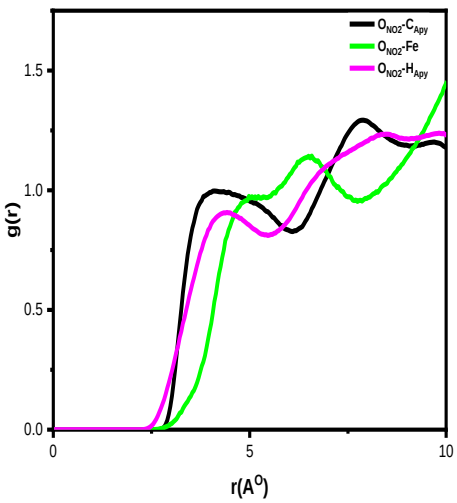
O_{NO2}-C_{Apy}
O_{NO2}-Fe
O_{NO2}-H_{Apy}
g(r)
r(A^O)

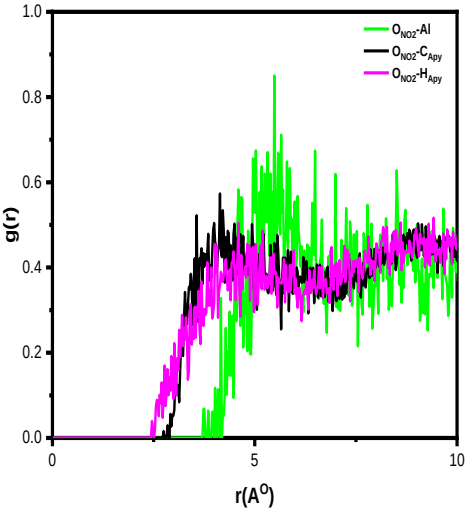
O_{NO2}-Al
O_{NO2}-C_{Apy}
O_{NO2}-H_{Apy}
g(r)
r(A^O)

(c) SO_2

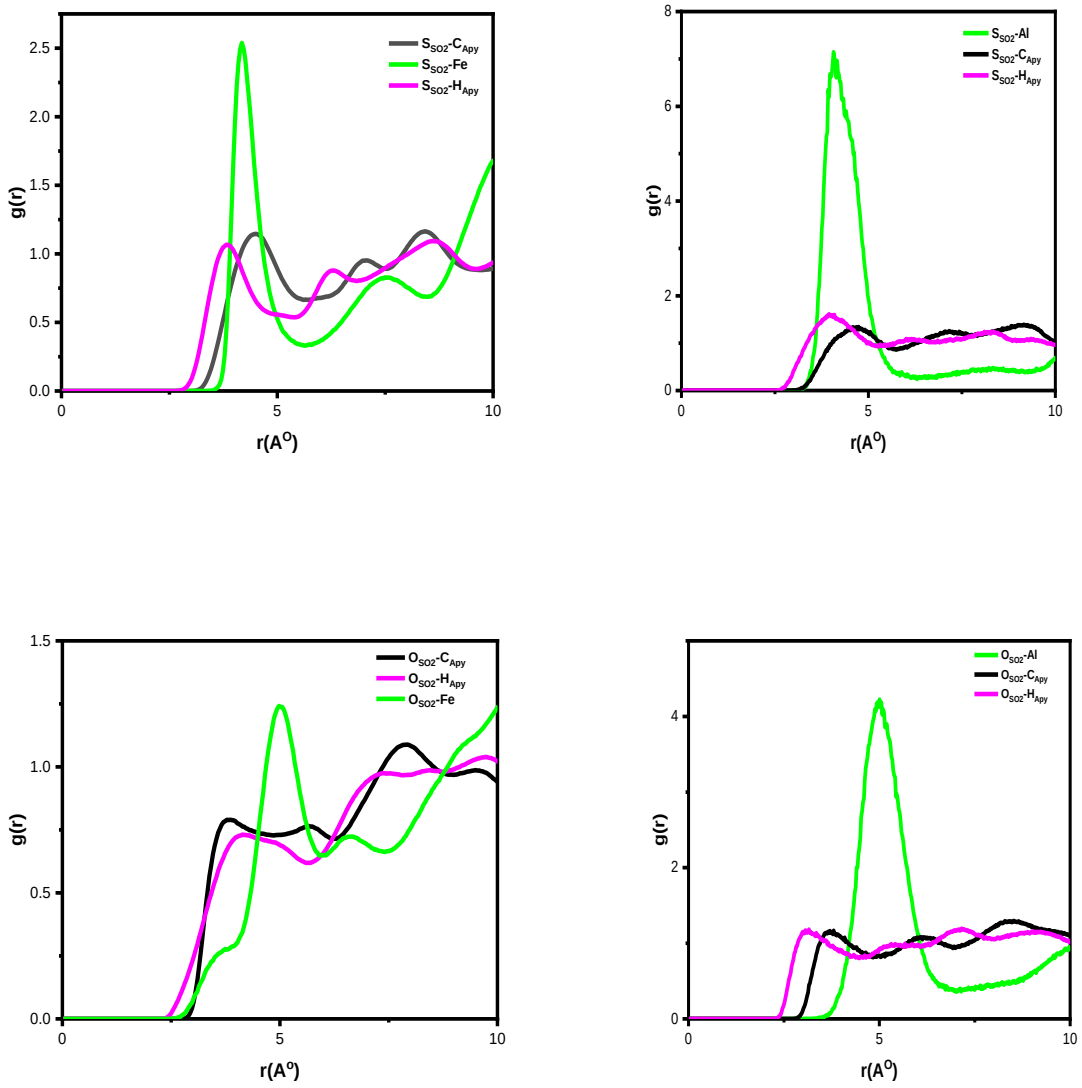

Figure S9: Radial distribution functions (RDF) between guest molecule and the atoms of the framework (C_{Azpy}: Black, H_{Azpy}: Magenta, Metal (Fe/Al): Green) extracted from the single component adsorption in FEFFIVE-Ni-Apy (left) and ALFFIVE-Ni-Apy (right) at 1 bar and 298 K

9. Acidic gas Conversion

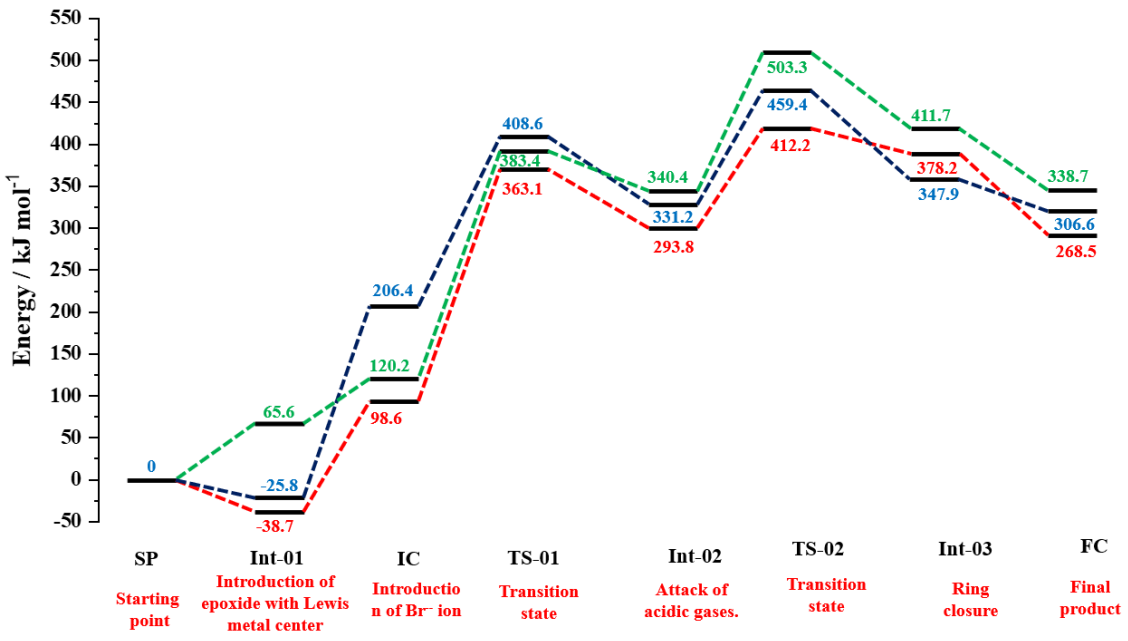

Figure S10: DFT energy profile diagram of acidic gases such as CO_2(red), SO_2(blue) and NO_2(green) using ALFFIVE square pillar moiety as a catalyst.

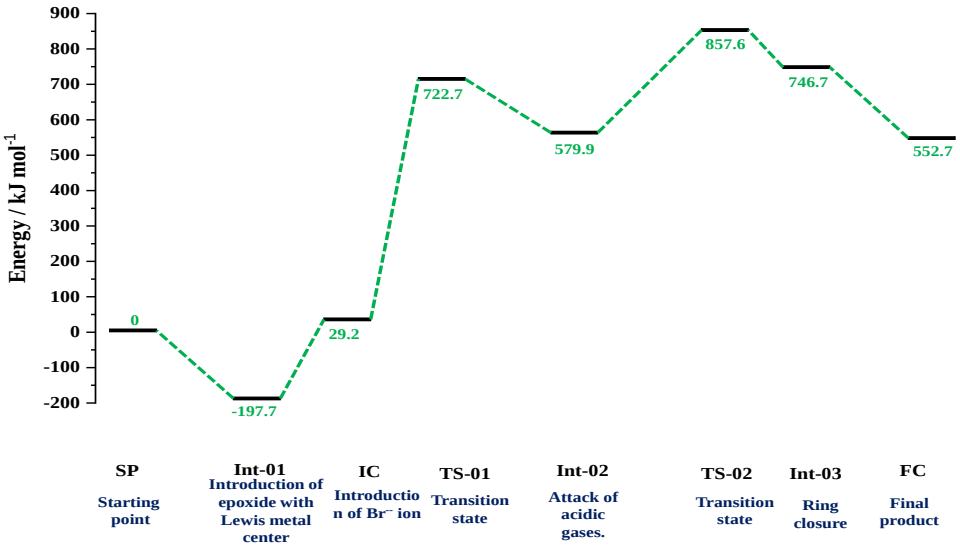

Figure S11: DFT energy profile diagram of NO_2 using ALFFIVE-Ni-apy as a catalyst.

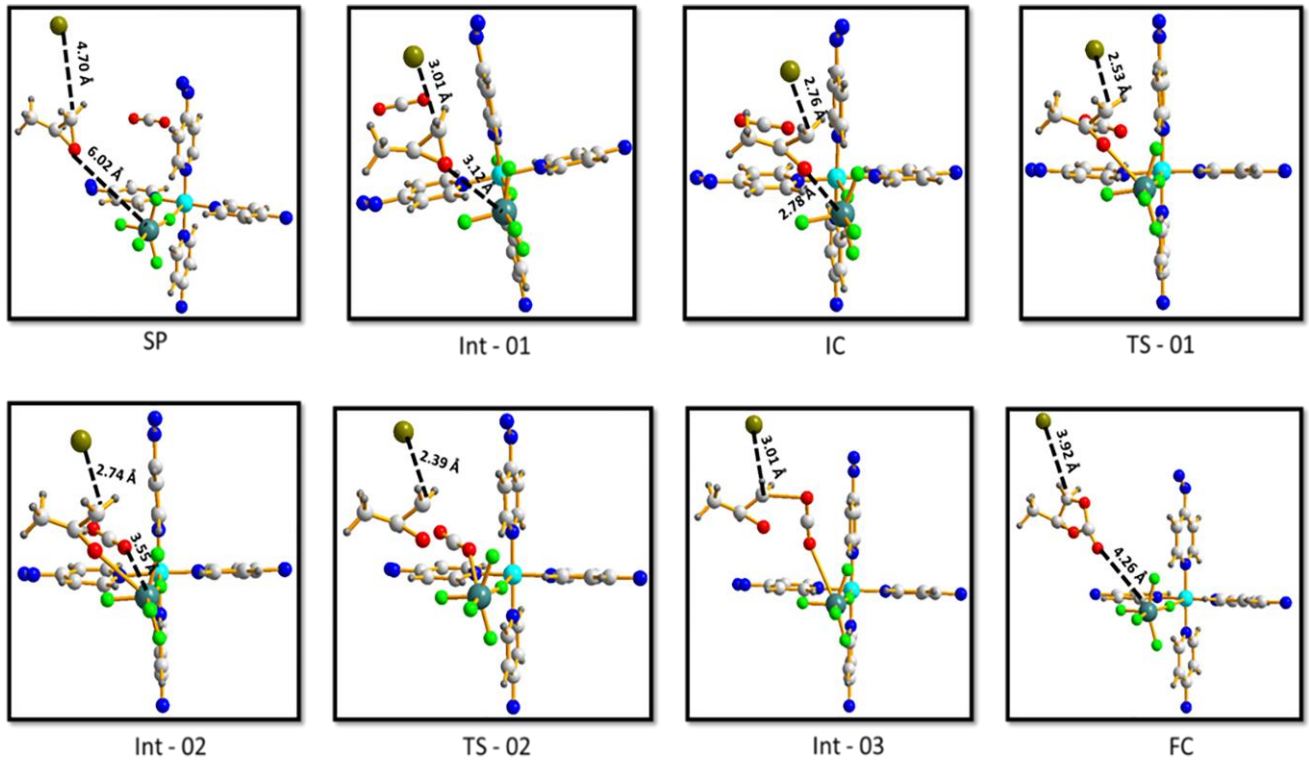

Figure S12. Pictorial representation of mechanism for CO_2 conversion using ALFFIVE-Ni-Apy as a catalyst.

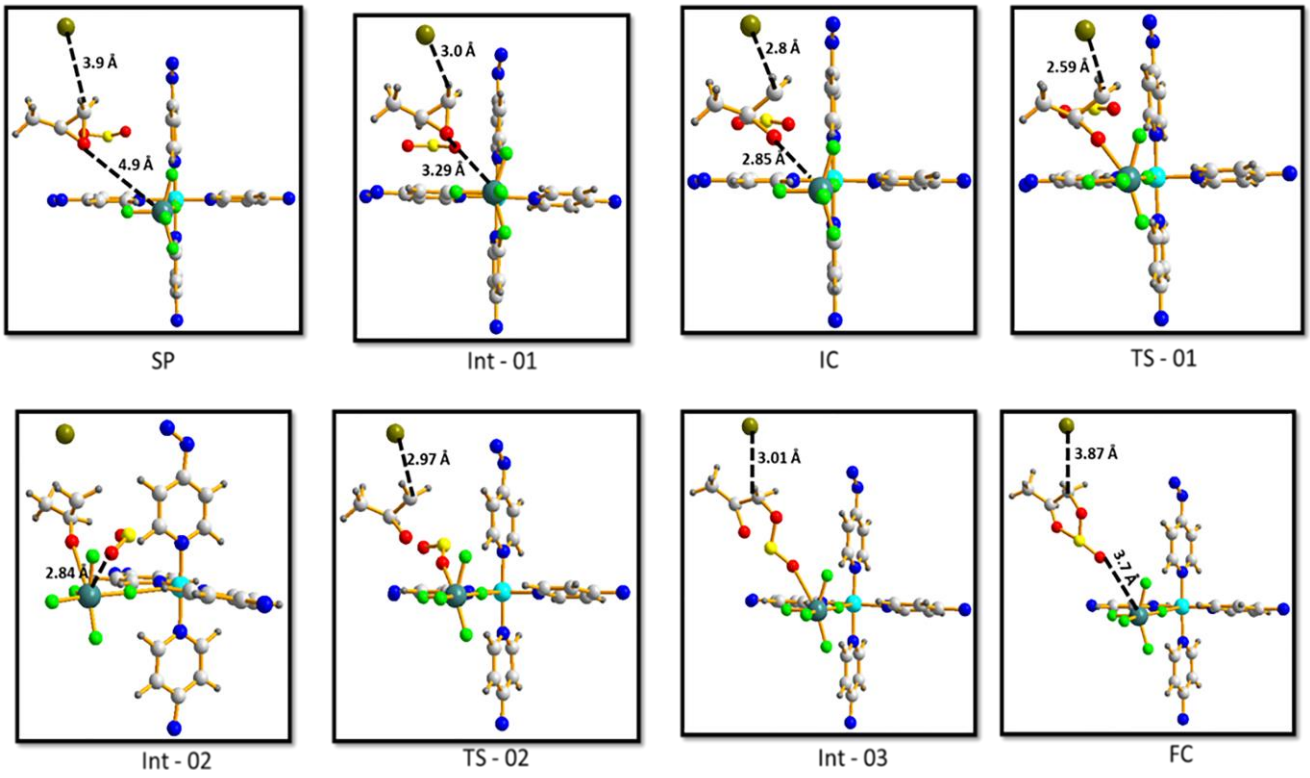

Figure S13. Pictorial representation of mechanism for SO_2 conversion using ALFFIVE-Ni-Apy as a catalyst.

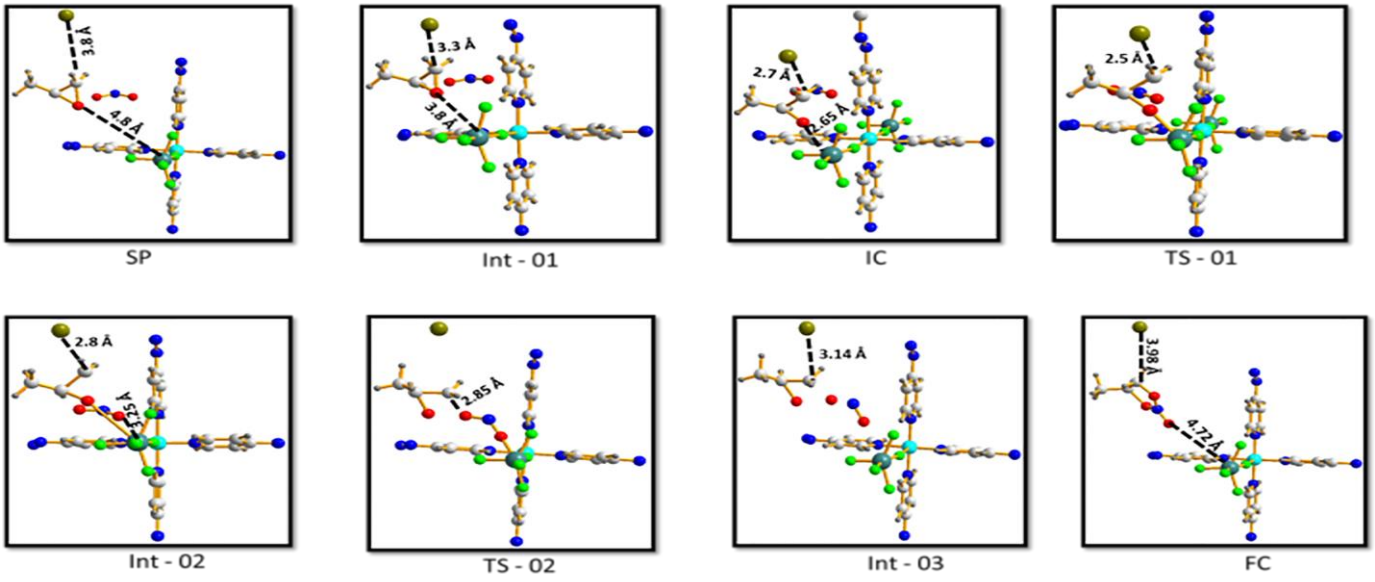

Figure S14. Pictorial representation of mechanism for NO_2 conversion using ALFFIVE-Ni-Apy as a catalyst.

10. Electronic charges of the atoms in the framework

Table S4: Electronic Charges of the atoms in the framework for the SO_2 catalytic fixation

Atom sites in ALFFIVE-Ni-Apy catalyst	Starting Point	Transition state – 01	Product
Aluminium metal (Open Metal site)	1.731204	1.632603	1.731694
Oxygen atom (Propylene Oxide)	-0.27184	-0.167555	-0.463211
Equatorial Fluorine of the pillar	-0.6682	-0.65808	-0.672963
Axial Fluorine of the pillar	-0.6317	-0.63484	-0.630890
Sulphur atom of the substrate	0.743273	0.680906	0.706515
Oxygen atom of the substrate	-0.342772	-0.322612	-0.409681

REFERENCE

1. J.P. Perdew, K.Burke and M. Ernzerhof. *Phys. Rev. Lett*. 1996, **77**, 3865−3868.

2. T. D. Kühne, M. Iannuzzi, M. D. Ben, V. V. Rybkin, P. Seewald, F. Stein, T. Laino, R. Z. Khaliullin, O. Schütt, F. Schiffmann, D. Golze, J.Wilhelm, S. Chulkov, M. H. BaniHashemian, V. Weber, U. Borstnik, M. Taillefumier, A. S. Jakobovits, A. Lazzaro, H. Pabst, T. Müller, R. Schade, M. Guidon, S. Andermatt, N. Holmberg, G. K. Schenter, A. Hehn, A. Bussy, F. Belleflamme, G. Tabacchi, A. Glöß, M. Lass, I. Bethune, C. J. Mundy, C. Plessl, M. Watkins, J. VandeVondele, M. Krack and J. Hutter, *J. Chem. Phys*., 2020, **152**, 194103–194150

3. K. Boguslawski, C.R. Jacob and M. Reiher. *J. Chem. Phys*. 2013 , **138**, No. 044111

4. J. VandeVondele and J. Hutter. *J. Chem. Phys*. 2007, **127**, No. 114105

5. S. Grimme, J. Antony, S. Ehrlich and H .Krieg. *J. Chem. Phys.* **2010**, 132, No. 154104

6. L.D.Gelb and K. E. Gubbins. *Langmuir*. **1998**, 14, 2097−2111

7. A.K. Rappé, C.J. Casewit, K.S. Colwell, W.A. Goddard and W.M. Skiff. *J. Am. Chem. Soc.* 1992, **114**, 10024−10035

8. S.L.Mayo, B.D. Olafson and W.A. Goddard. *J. Phys. Chem. A*.1990, **94**, 8897−8909.

9. J.G.Harris and K.H. Yungt. *J. Phys. Chem. B.* **1995**, 99, 12021−12024

10. E. Bourasseau, V. Lachet, N. Desbiens, J.B. Maillet, J. M. Teuler, P. Ungerer. *J. Phys. Chem. B* .2008, **112**, 15783-15792

11. M.H. Ketko, G. Kamath, J.J. Potoff. *J. Phys. Chem. B* .2011**,115**, 4949-4954

12. D. Dubbeldam, S. Calero, D.E. Ellis, and R.Q. Snurr. *Mol. Simul*. 2016, **42**, 81−101

13. B.A.Wells and A.L. Chaffee. *J. Chem. Theory Comput*.2015, **11**, 3684−3695

14. D.-Y. Peng and D.B. Robinson. *Ind. Eng. Chem. Fundam*. **1976**, 15, 59−64

15. T.J.H. Vlugt, E. García-Perez, D. Dubbeldam, S. Ban, S. Calero. *J. Chem.Theory Comput*. 2008, **4**, 1107−1118